Probing the Structure of Long Single-Stranded DNA Fragments with Neocarzinostatin Chromophore. Extension of the Base-Catalyzed Bulge-Specific Reaction†

Adonis Stassinopoulos and Irving H. Goldberg*

Department of Biological Chemistry and Molecular Pharmacology, Harvard Medical School, Boston, Massachusetts 02115

Received August 2, 1995®

ABSTRACT: The base-catalyzed (bc) thiol-independent cleavage reaction of neocarzinostatin chromophore (NCS chrom) has been characterized with long single-stranded (ss) DNA in order to use this reaction as a selective probe for the tertiary structure of naturally occurring ss nucleic acids. The ss circular $\phi\chi$ 174 phage and M13mp18 phage DNAs (~5000 and 7500 bases, respectively) were shown to be bc NCS chrom reaction substrates, exhibiting the expected pH dependence. The ss DNA fragments (150−450 bases) were cleaved at six major sites; the lesions occurred at T-rich non-double-stranded sequences, as predicted from comparison with the minimal energy secondary structures. These sites exhibited the expected pH and drug: DNA ratio dependence shown to be required for this reaction. Optimization of the shortest sequence, which gave the highest cleavage yield, identified the minimal sequence requirements for the site (19-mer of the sequence 3′TACTGAGTCTCCTTTTGTA5′, attacked residue in bold). Folding pattern analysis predicted that the oligonucleotide contained a two-base bulge at the cleavage site; this result was consistent with the observation that removing features which destabilize the bulged structure increased the cleavage yield. Furthermore, the derived 19-mer was shown to generate maximal amounts of the final drug product of the bc DNA cleavage reaction. Reaction of an RNA 339-mer containing the same sequence as one of the long ss DNA fragments showed it not to be a substrate for the bc reaction, while similar results were obtained for the RNA analog of shorter oligodeoxyribonucleotides identified in this and earlier studies. Through a combination of thermodynamic and kinetic assays, the observed difference in reactivity was shown to be the result of the low binding of the cleaving species to RNA.

Neocarzinostatin chromophore (NCS chrom: Scheme 1, **1**) (Ishida et al., 1965; Goldberg, 1991, and references therein; Goldberg & Kappen, 1994, and references therein) is the prototype of the anticancer enediyne antibiotics. NCS chrom exists in nature as a 1:1 complex (holo-NCS) with its host protein (apo-NCS). Its mode of action *in vivo* is believed to be through oxidative damage of chromosomal DNA after activation by glutathione (GSH) inside cells. The specificity of its binding and reactivity with double-stranded (ds) DNA in the presence of thiols has been studied extensively (Goldberg, 1991, and references therein; Goldberg & Kappen, 1994, and references therein). Reactivity has also been reported in the presence of GSH with unusual ds DNA structures, such as those containing one-base bulges, mismatches, and wobble base pairs (Williams & Goldberg, 1988; Kappen & Goldberg, 1992a,b).

Chromophore activation by thiols occurs through a nucleophilic attack at C12, which results in the formation of the cumulene **2**. The labile cumulene undergoes a spontaneous Bergman-like cyclization to the biradical **3**, which after abstraction of H atoms from DNA becomes the stable aromatic postactivated form **4** (Scheme 1) (Hensens et al., 1983; Myers, 1987; Myers & Proteau, 1989). **4** has been used successfully as a stable drug analog to study the binding at specific ds damage sites located on single site-containing oligonucleotides (SSO) (Stassinopoulos & Goldberg, 1995).

Scheme 1: Proposed Mechanism for the Activation of NCS Chrom by Glutathione

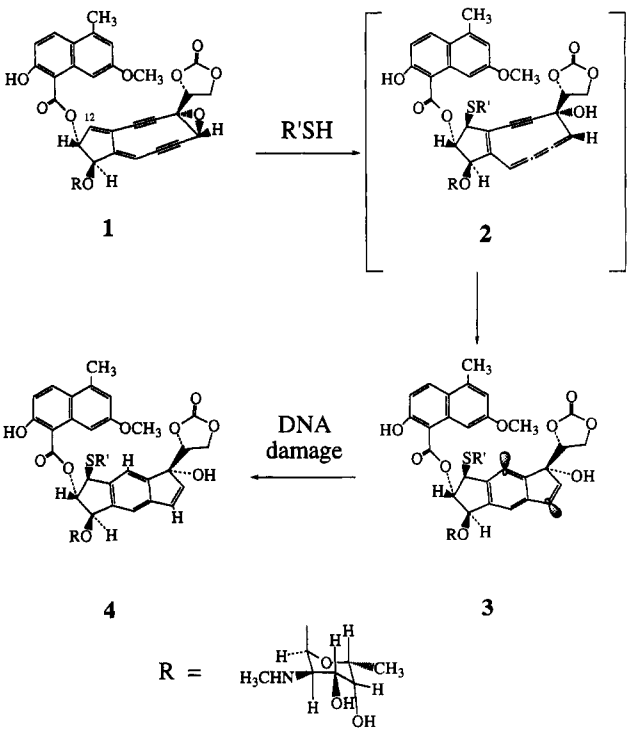

A complex of **4** with an SSO has been structurally characterized through ^{1}H NMR spectroscopy (Gao et al., 1995a,b).

† This work was supported by U.S. Public Health Service Grant CA 44257 from the National Institutes of Health.

* To whom correspondence should be addressed.

® Abstract published in *Advance ACS Abstracts,* November 1, 1995.

0006-2960/95/0434-15359$09.00/0 © 1995 American Chemical Society

Scheme 2: Proposed Mechanism for the Intramolecular Activation of NCS Chrom at Basic pH in the Absence or Presence of Bulged DNA

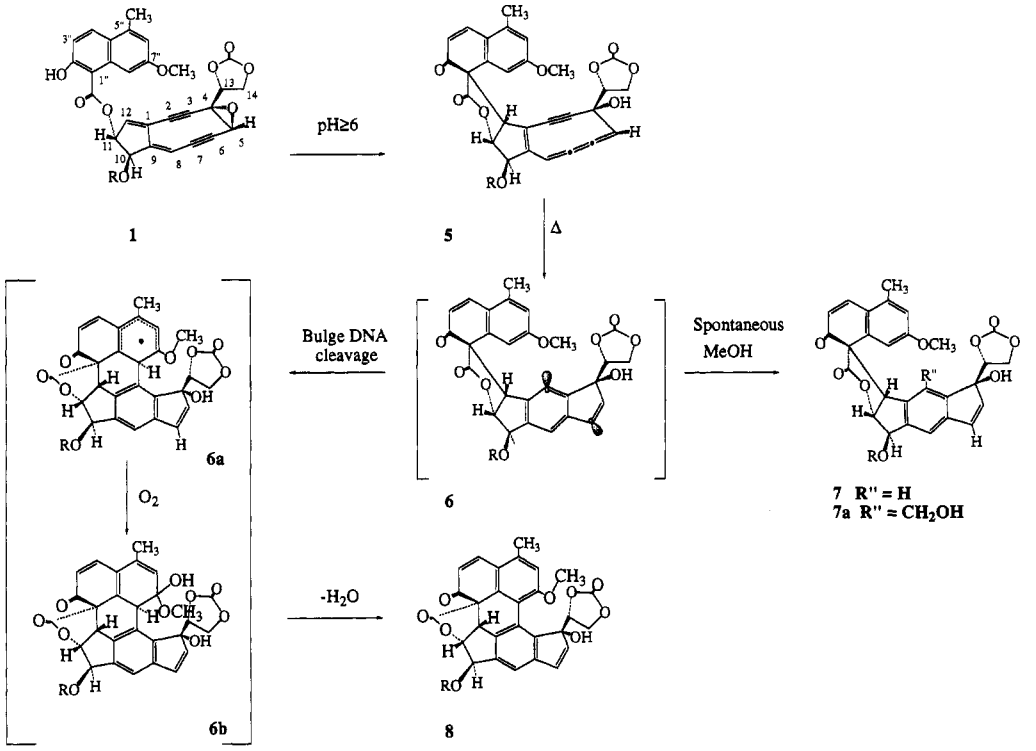

Recently, a novel mode of intramolecular base-catalyzed (bc) drug activation has been reported in the presence of an oligonucleotide containing a two-base bulge (Kappen & Goldberg, 1993a,b, 1995). This reaction results in the specific cleavage at one bulged residue. During this activation, instead of the thiol attack at C12, an intramolecular Michael addition of the phenol enolate at C1″ to C12 has been proposed, to give cumulene **5** (Scheme 2). Cumulene **5** undergoes a Bergman-like rearrangement to the biradical **6**, which is in turn responsible for the 5′ H abstraction from the attacked residue and attack at the C8″ of the naphthoate group. The biradical **6** transforms into the aromatic compound **8**, through the proposed intermediacy of the radical **6a** and compound **6b** (Hensens et al., 1993, 1994). This novel mode of NCS chrom activation for bulged DNA cleavage is connected to the spontaneous drug inactivation in aqueous solutions at physiological pHs, which results in the alternative products of the biradical **6**, compound **7** and **7a** (Povirk & Goldberg, 1980; Napier & Goldberg, 1982; Hensens et al., 1993, 1994).

Subsequent binding studies have shown that, of the stable structural analogs of the biradical **6** and radical **6a** (compounds **7** and **8**, respectively), only compound **7** binds to a substrate bulged DNA in a site-specific manner (Yang et al., 1995). This indicates that the damage-causing reaction results from the formation of a specific complex between the bulged structure and the biradical **6** or the cumulene **5** (Figure 1) and implies that the reaction may be used as a selective probe of the tertiary structure of single-stranded (ss) nucleic acids containing the appropriate bulges. Since it was shown that this mode of activation does not result in the cleavage of, or binding to, ds DNA regions (Yang et al., 1995), this kind of DNA cleavage is expected to occur less frequently and at ss regions flanked by the ds regions, attacked in the presence of thiol.

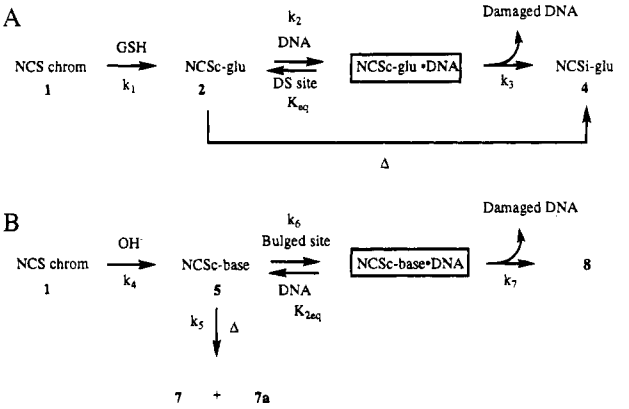

FIGURE 1: Reaction schemes for (A) the GSH activation of NCS chrom, resulting in DNA cleavage, and (B) the base-catalyzed activation of NCS chrom, resulting in bulge-specific DNA cleavage. k_n is the reaction rate for step n, and K_{eq} is the equilibrium constant for the formation of a noncovalent complex. NCSc-glu is the GSH-generated cumulene **2**, and NCSc-base is the base-generated cumulene **5**. DS site is a ds DNA cleavage site, leading to ss or ds lesions. Bulged site is a non-ds DNA site where, upon bc activation, a ss lesion occurs. Δ denotes a thermodynamically spontaneous reaction.

In this paper, the bc cleavage reaction of NCS chrom has been further characterized with biologically relevant and naturally occurring circular ss phage DNAs (virions, ~5000 and 7500 bases) (Denhardt et al., 1978), as well as long fragments of ss DNA (150−450 bases), as substrates. Although specific cleavage sites were identified for the DNA fragments, RNAs with the same sequences and potentially containing the same sites were found to be undamaged by NCS chrom under the same reaction conditions.

On the basis of spectroscopic experiments in the absence and presence of SSOs for the bc reaction, identified by earlier

studies (Kappen & Goldberg, 1993a,b, 1995), we were also able to explain the dynamics controlling the outcome of the competition between the bc decomposition of NCS chrom and the bc ss DNA cleavage by NCS chrom (Figure 1). Through these experiments, we found that the nonreactivity of RNA is related to a much lower binding affinity of the cleaving species for RNA sites.

MATERIALS AND METHODS

T4 kinase, alkaline phosphatase, and T4 RNA ligase were purchased from New England Biolabs. TaqI polymerase, NTPs, and Ampliwax were purchased from Perkin-Elmer. T7 RNA polymerase, recombinant RNasin, and NTPs were purchased from Promega. The ss M13 phage DNA and ss and ds $\phi\chi$ 174 phage DNA were purchased from New England Biolabs. γ-[^{32}P]ATP and [^{32}P]Cp were purchased from New England Nuclear. Polyacrylamide gels were prepared by the use of the Sequagel system from National Diagnostics. Low-melting point agarose, "100-base pair markers", and G-25 Sephadex columns were purchased from Pharmacia. Avidin immobilized on agarose beads was purchased from Spectrum. Diethyl pyrocarbonate was purchased from Aldrich.

Buffer solutions and water used in the RNA experiments were treated with diethyl pyrocarbonate and autoclaved before use. Appropriate precautions for the avoidance of RNAse contamination were taken (Ausubel et al., 1989).

Denaturing gels were run in a 1 × TBE (Tris borate EDTA; Ausubel et al., 1989) buffer at room temperature and 1500 V. Native polyacrylamide gels were run in 1 × TBE buffer (pH ≈ 8.5) at 4 °C and 600 V. Agarose gels of the appropriate percentage were run in 1 × TBE buffer (pH ≈ 8.5) at room temperature and 100 V.

Neocarzinostatin was purchased from Kayaku Chemicals. NCS chrom was isolated according to the published procedure and stored as a methanolic solution at −70 °C (Kappen & Goldberg, 1992a). NCS chrom spontaneous decomposition product **7** was synthesized by incubation of NCS chrom at pH 8.5, according to the published procedure (Hensens et al., 1994). **7** was high-performance-liquid chromatography (HPLC) purified on a reverse phase C18 column (Dynamax 300A, Rainin) under the conditions described earlier (Hensens et al., 1994).

Standard NCS chrom reaction conditions were the same as the ones described before (Kappen & Goldberg, 1992a, 1993a,b).

Standard phosphoramidites and Bioteg and T-Bio phosporamidites, as well as solvents and reagents for DNA and RNA synthesis, were purchased from Glen Research. CPG columns were purchased from CPG Inc.

Oligodeoxyribonucleotides were synthesized on an ABI 300A synthesizer. They were then deprotected under standard conditions with 14 M ammonia and precipitated with nBuOH. Concentrations were determined using the additive extinction coefficients method (Cantor & Warshaw, 1970). They were then used without further purification. Oligoribonucleotides were chemically synthesized either on the ABI synthesizer or by "runoff transcription" using T7 RNA polymerase, the appropriate primer, and a ds template (Milligan et al., 1979). The templates were synthesized by the use of the PCR reaction. Chemically synthesized oligoribonucleotides were deprotected with concentrated ammonium hydroxide in methanol (1:3). They were then desalted with the use of a G-25 Sephadex column and the fractions collected, concentrated, and treated with tetrabutylammonium fluoride to remove the 2′-OH protecting group. Finally, they were desalted through another cycle of purification on a G-25 Sephadex column. Oligonucleotides were 5′ end-labeled with γ-[^{32}P]ATP and T4 kinase under standard conditions. Ribonucleotides were 3′ end-labeled by the use of T4 RNA ligase and [^{32}P]Cp (Ausubel et al., 1989).

PCR reactions were carried out under standard conditions (Ausubel et al., 1989), using the hot-start method and Ampliwax on a Perkin-Elmer DNA thermal cycler. The AP1−3 variant of a pUC19 plasmid (Dedon & Goldberg, 1992) was used as the template. More specifically, the reactions were carried out in a total volume of 100 μL, in 1 × TaqI buffer, in the presence of 200 μM NTPs and 1 μM each of the two primers. Template (125 μg) and TaqI (2.5 units) were used in each reaction. The $MgCl_2$ concentration was optimized for each set of primers. Each PCR cycle consisted of 1 min at 94 °C, 2 min at 55 °C, and 1 min at 72 °C. The number of cycles giving the optimum yield was found experimentally (30−45). The products of the PCR reaction were analyzed by the use of a 2% agarose gel and their size compared to the 100-base pair markers purchased from Pharmacia. The yield of product per tube depended on the size of the product and was between 1 and 5 μg of DNA. Sequences for the PCR primers used were as follows: BioP1, 3′-BCAGCTGGCACTACAG; BioP6, 3′-BCTTCCGGCTCGTATG; BioP2, 5′-TAACGCCAGGGTTTT; BioP3, 5′-CCGCTCTAGAACTAG; BioP4, 5′-TACCGTCGACCTCGA; and BioP5, 5′-TTGTTATCCGCTCAG. B stands for the biotinylated nucleotide, either BioTeg or T-Bio.

In order to separate the two strands of the PCR products, a biotinylated primer was used for the (−) strand. The biotinylated primer was synthesized by standard phosphoramidite technology and the use of either the biotin-linker phosphoramidite Bioteg or the T-Bio phosphoramidite at the 3′ end, in order to insert a biotinylated T residue near the 3′ end.

To generate ss fragments of DNA from the ds DNA fragments bearing a biotin tag on one of the two strands, a solution of the PCR product was incubated with a 1.1 molar excess of avidin immobilized on agarose for 25 min at 37 °C. The resulting slurry was centrifuged, and the supernatant was decanted. The beads of agarose were then washed twice with 50 mM Tris·HCl (pH ≈ 7.5) and 100 mM NaCl buffer, and the supernatant was again decanted and discarded. The agarose beads were subsequently incubated with 200 μL of 150 mM NaOH solution for 5 min to "melt" the hydrogen bonds between the two strands. The supernatant, containing the nonbiotinylated strand, was thereby separated from the strand containing the biotin tag which was bound on the agarose beads. Treatment with NaOH and centrifugation were repeated once more, and the two supernatants were combined. The solution was neutralized with 1.1 equiv of acetic acid, and an additional amount of 3 M NaOAc was added to a final [NaOAc] = 0.3 M. The ss DNA was finally precipitated by the addition of 500 μL of EtOH, incubation at −70 °C for 20 min, and centrifugation (14 000 rpm, 30 min). The precipitate was washed two times with 70% EtOH and one time with 100% EtOH, centrifuged (14 000 rpm, 15 min), and briefly dried. It was then taken up in the

appropriate buffer, to give a solution of ss DNA fragment of the desired sequence. The fragments synthesized by this procedure were proven to be of the expected length and pure by either nondenaturing agarose or denaturing polyacrylamide gels.

Runoff transcriptions were carried out under standard conditions (Ausubel et al., 1989) in the presence of recombinant RNasin to prevent ribonuclease digestion (Promega technical manual, revised December 1993). The T7 required primer sequence was incorporated in the ds template synthesized by the PCR reaction (Milligan et al., 1979). The RNA was analyzed and further purified by the use of a denaturing gel. The gel band corresponding to the RNA of interest was visualized, excised, crushed, and soaked in RNAse-free water to retrieve it.

Calculations of the rates of NCS chrom decomposition from the fluorescence increase at 550 nm were carried out in the same manner as that used by Dedon and Goldberg (1992). The plot of $\ln(100-F_t)$ *vs* time was fitted to the equation

$$\ln(100-F_t) = \ln(100-F_0) - Kt \qquad (1)$$

where F_t is the fluorescence at incubation time t and F_0 is the fluorescence value at $t = 0$. The initial rate constant for the pseudo first order of the NCS chrom disappearance was equal to the slope of the line.

Binding constants for the binding of **7** to the bulge oligonucleotides were derived from the same Scatchard equation as reported previously (Yang et al., 1995).

In order to calculate the percent yield of the cleavage reactions, the products were resolved on a denaturing gel. The appropriate bands were then analyzed with the use of a PhosphorImager screen (Molecular Dynamics) and a Molecular Dynamics PhosphorImager SP. The integrations of the bands were performed as volume integrations using the ImageQuant v 3.4 software, and the cleavage yields were the percentage of counts for a particular band *vs* the total counts on each lane.

RESULTS AND DISCUSSION

Reactivity Characteristics of the Base-Catalyzed Reaction with Single Site-Containing Oligonucleotides

The bc bulge-specific reaction of NCS chrom with ss DNA is intimately connected to its spontaneous decomposition under physiological conditions (Figure 1). In order to use this cleavage mode as a selective probe of the tertiary structure of ss nucleic acids, it is important first to decipher the reaction characteristics in the presence or absence of SSO substrates for the bc reaction.

(a) Reaction Rate. The spontaneous inactivation of NCS chrom in aqueous solution has been shown in the past to be a very facile reaction, leading to the formation of a highly fluorescent mixture of products, coined chromophore D (Povirk & Goldberg, 1980; Napier & Goldberg, 1982). This crude mixture is now known to be composed of mostly **7** and to a lesser extent **7a** (Figure 1, step 5) and their decomposition products (Hensens et al., 1993, 1994). The bc transformation of NCS chrom, which can be conveniently followed by the increase of fluorescence at 550 nm (λ_{exc} = 400 nm), has been shown to be influenced by the presence of either excess ds DNA or equimolar amounts of apo-NCS.

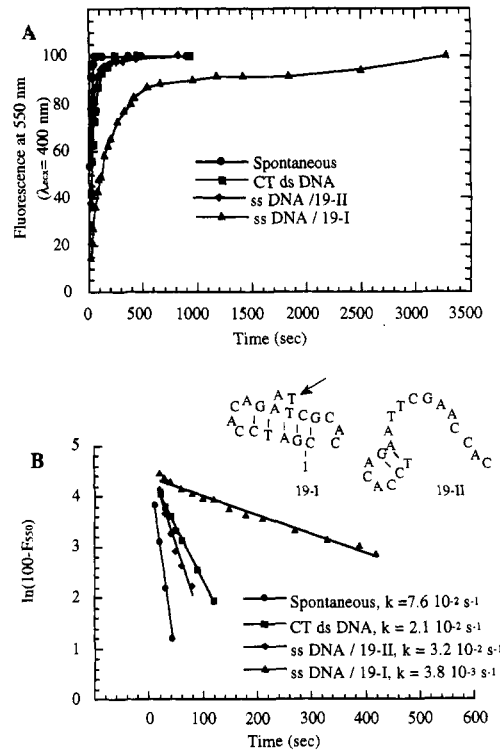

FIGURE 2: (A) Plot of the fluorescence at 550 nm (λ_{exc} = 400 nm) *vs* the time of incubation. Conditions: 5 μM NCS chrom in 50 mM Tris·HCl (pH = 8.5) and 10% MeOH (●) alone, (■) with 180 μM (phosphate) calf thymus DNA, (▲) in the presence of 2 equiv (10 μM) of substrate 19-I oligonucleotide, and (◆) in the presence of 2 equiv (10 μM) of nonsubstrate 19-II oligonucleotide. 19-I is 5′CGATCCACAGAATTCGCAC3′, and 19-II is 5′TCCACAGAATTCGCACCAC3′. The predicted secondary structures calculated by the program MFOLD are shown as an insert. The arrow denotes the site of cleavage. (B) Initial rates of chromophore inactivation calculated from the linear eq 1.

In both cases, this effect can be explained by invoking interference with the initiation step of the spontaneous decomposition reaction.

Addition of ds DNA has been shown to slow down this inactivation reaction to some extent without altering its final result (Figure 2) (Povirk & Goldberg, 1980). This decrease is presumably the immediate consequence of the NCS chrom intercalation in ds DNA, which results in inhibition of the C1″ attack on C12 (Scheme 2). As one can extrapolate from the recent ^{1}H NMR structure of an SSO with **4** (Gao et al., 1995a,b), during intercalation, C1″ and C12 become physically separated by the aromatic systems of the DNA bases, as C1″ is located between the aromatic bases in the intercalation site, while C12 is located in the minor groove (Gao et al., 1995). The nucleophilic attack/Michael addition initiating the inactivation reaction can, thus, only happen through the free NCS chrom (Figure 1). Since only a small amount of NCS chrom is free ($K_d \approx 1-5$ μM), the observed reaction rate is slower.

A similar rationale can also account for the stability of NCS chrom, when bound in the 1:1 holo-NCS complex. In this case, as revealed in the recent crystal structure (Kim et al., 1993), not only is **1** "locked" in an unfavorable conformation for the C1″−C12 Michael addition to occur, but also a Phe ring physically blocks the required attack by C1″ on C12. This explanation, and the high binding constant ($K_d \approx 10^{-8}$ M) of the apo-NCS for NCS chrom, accounts for its long lifetime as a holo-NCS complex under physi-

ological conditions (Goldberg, 1991, and references therein; Goldberg & Kappen, 1994, and references therein).

The fluorescence increase at 550 nm was found to become much slower in the presence of a bulge-containing substrate oligonucleotide [19-I, Figure 2 (Kappen & Goldberg, 1993b)], demonstrating a slower reaction rate for the decomposition of NCS chrom. As deduced by the HPLC analysis of the reaction products at the end of the reaction, the decrease in rate occurs because the spontaneous reaction leading to **7** (and **7a**) is almost completely inhibited, while there is a slower production of fluorescent product **8** ($k_7 \ll k_5$, Figure 1). Indeed, in the case of a reaction in the presence of 19-I, **8** can be detected as the major reaction product with the concomitant disappearance of all but traces of **7** and **7a**. Moreover, **8** is the major fluorescent species present in the spent reaction mixture, when a substrate oligonucleotide is included. Given that the extinction coefficients for all three products are of the same order of magnitude, the fluorescence increase at 550 nm in the presence of a bulge-containing oligonucleotide can only be due to the formation of **8**. This rate of fluorescence increase ($k_f = 3.8 \times 10^{-3}$ s^{-1}) was found to be very similar to the rate of the bc ss DNA cleavage reaction ($k_c = 1.07 \times 10^{-3}$ s^{-1}) (Kappen & Goldberg, 1993b). The similarity of the rates establishes a kinetic connection of the fluorescence increase due to **8** production and the cleavage at the bulge sites. In a control experiment, the presence of a nonsubstrate ss oligonucleotide [19-II, Figure 2 (Kappen & Goldberg, 1993b)] was shown not to retard the fluorescence rate increase in a similar manner or alter the products of the reaction (Figure 2A,B). On the basis of the proposed mechanism for the bc reaction (Scheme 2, Figure 1), the most plausible explanation for the slow rate of both the DNA cleavage and the drug decomposition is that either the hydrogen abstraction from the oligonucleotide and/or the C8″−C2 bond formation steps are rate-determining, although a DNA-induced electronic stabilization of the cumulene cannot be excluded. Nonetheless, for one to explain the slow step 7 competing efficiently with the fast side reaction step 5, one would have to invoke that the cleaving complex for this reaction, **5**•DNA (Figure 1), has a slow off rate for the cumulene. This is equivalent to a high binding constant for the previously mentioned complex (K_{2eq} is less than micromolar). The dissociation constant K_{2eq} will have to be lower by at least 1 order of magnitude than the one measured for the stable complex formation of a substrate oligonucleotide and **7** (Yang et al., 1995). A similar situation has been found for the GSH-activated reaction from comparisons between affinity cleavage methods that measure K_{eq} (Figure 1) and binding studies of the stable drug analog **4** (Stassinopoulos & Goldberg, 1995).

(b) Effect of the NCS Chrom Concentration on the Final Yield of Cleavage. Incubation of a fixed amount of the bulge-containing, 16-mer oligonucleotide 5′CGATCCACA-GAA**T**TCG3′ (Table 1; site A, predicted folding in the insert of Figure 3) with increasing amounts of NCS chrom in a bc "affinity cleavage"-type experiment did not show the expected concentration/cleavage relation (Figure 3) (Stassinopoulos & Goldberg, 1995, and references therein). Unlike ds single site-containing oligonucleotides for the GSH activation reaction, the bc cleavage yield did not reach a plateau at high drug concentrations, indicating saturation of the cleavage site by the binding/cleaving species (Stassinopoulos & Goldberg, 1995). Instead, the cleavage yield

Table 1: Lesion Sites for the Single-Stranded Long DNA Fragments

site	sequence (3′−5′)[a]	position[b]	fragment exhibiting the lesion[c]	study
A	GCTTAACG	NA[d]	NA	LK1[e]
B	CGAG**TTT**AGACC	NA	NA	LK2
1	TTGT**T**TTCGAC	214	I, II	this work
2	TAGCTTAAGTT	269	I, II, V	this work
3	CTCCT**T**TTGTAT	290	I, II	this work
4	GAGCA**T**ACAAC	131	III	this work
5	AAGTGTGTCCT	165	III	this work
6	TATGCTTAAGG	224	V	this work

[a] Attacked residue shown in bold. [b] Numbers correspond to the numbering scheme of Figure 6. [c] Names of the fragments from Figure 6. [d] NA stands for not applicable. [e] LK1 refers to Kappen and Goldberg (1993a,b); LK2 refers to Kappen and Goldberg (1995).

increased, reached a maximum, and decreased again, with the concomitant formation of a new band(s) moving slower than the intact oligonucleotide (Figure 3). Observation of this band(s) ("Adduct" in Figure 3) is consistent with the formation of products from covalent modification of the original oligonucleotide, including cross-links. This behavior, where an excess of the native drug seems to alter the reactivity and decrease the yield of direct damage, is consistent with either destruction of the binding site's tertiary structure by intercalation of multiple molecules of the native chromophore **1** or competition of the spontaneous product **7** for the site (Yang et al., 1995). **7** has indeed been found to inhibit the cleavage reaction with a K_i of 5.4 μM. This would not, however, explain the formation of the observed adduct band, as the formation of this band was not found during the inhibition experiments (Yang et al., 1995). Whichever the explanation, this behavior has been observed for a series of substrates and seems to be a characteristic of the interactions for the bc reaction of NCS chrom. Its practical implication is that, in order to obtain the maximum cleavage possible for a bc reaction site, one needs to find the optimum concentration of NCS chrom, as an excess of drug will inhibit the observable cleavage reaction.

(c) pH Dependence. The bc cleavage of bulged oligonucleotides by NCS chrom increases as the pH of the solution becomes higher, reaches a maximum at pH $\approx$ 8.5, and then decreases at pH > 9, while being markedly inhibited by pH $\approx$ 5 (Kappen & Goldberg, 1992b). The spontaneous decomposition reaction behaves as a pseudo-first order base-catalyzed reaction, the rate of decomposition increasing linearly with pH (Figure 4). The reason the cleavage reaction is inhibited at low pH values is that the equilibrium of the phenolate deprotonation responsible for the Michael addition lies toward the protonated form at that pH (pK_a of phenol $\approx$ 8.5). This precludes the formation of the cumulene **5** and cleavage of DNA.

At pHs > 9, the spontaneous decomposition rate becomes faster, but the cleavage yield gets reduced. If the mechanism of Figure 1B is correct and there is a common intermediate for the bc DNA cleavage and the spontaneous decomposition (NCS-base **5**), the cleavage yield reduction may only be attributed to a destabilization of the binding pocket and/or a pH-induced structural rearrangement of the residues at the bulged region. If a decomposition mechanism operates at higher pHs, which does not bear a common intermediate with the spontaneous decomposition pathway (step 5), it could compete with the DNA cleavage reaction and inhibit the

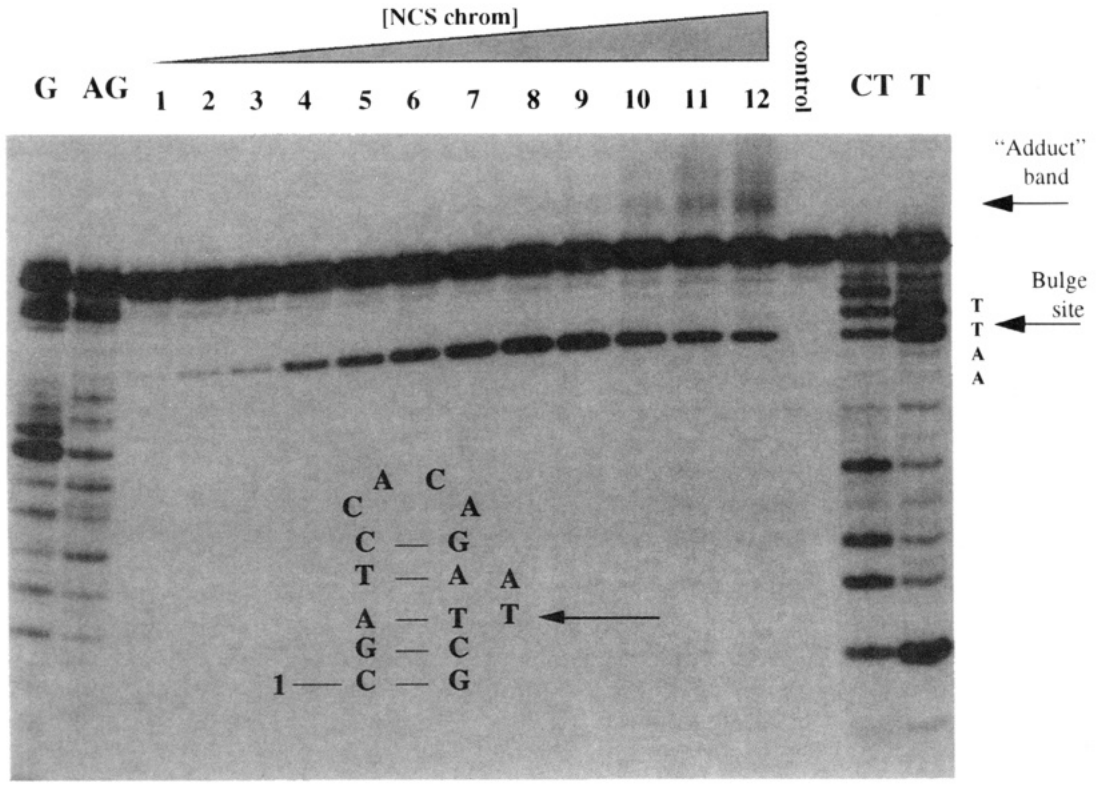

FIGURE 3: Gel analysis of the cleavage for the substrate 16-mer 5′CGATCCACAGAA**T**TCG3′ (attacked residue in bold), at different NCS chrom concentrations. Arrows denote the cleavage site and the adduct band. Electrophoresis was on a 20% denaturing polyacrylamide gel. G, AG, T, and CT denote Maxam−Gilbert chemical markers. Lanes 1−12: cleavage reactions of carrier-free 16-mer with 15.5, 32.5, 67.5, 155, 325, and 675 nM and 1.55, 3.25, 6.75, 15.5, 32.5, and 67.5 μM, respectively, NCS chrom (final). Incubation: 1.5 h at 4 °C in 50 mM Tris·HCl (pH = 8.5) and 10% MeOH. Control denotes a reaction with no NCS chrom included. Insert shows the predicted secondary structure for the 16-mer.

cleavage at higher pH values. This however is inconsistent with the observation that no significant amounts of other inactivation products are produced at higher pH values except for **7**, **7a**, and their decomposition products, as deduced by HPLC analysis of the spent reaction mixtures at higher pH values (A. Stassinopoulos and I. H. Goldberg, unpublished results).

Reactions with Circular Single-Stranded Phage DNAs

The ss phage DNA is a substrate for the bc NCS chrom reaction. Reactions of NCS chrom with the ss circular virions of $\phi\chi$ 174 and M13mp18 phages were conducted under the standard conditions of the bc reaction. These large circular DNAs, ~5000 and 7500 bases long (Denhardt et al., 1978), respectively, were expected to have several cleavage sites. A series of different drug concentrations were tested to find the optimum one (Figure 5). The results observed were the same for both $\phi\chi$ 174 and M13mp18 phage ss DNAs, but because of its convenient smaller size, only $\phi\chi$ 174 will be considered. No significant damage was observed for low ratios of drug:DNA (ratio in moles of drug per moles of phosphate, $d/P = 4$; ratio in moles of drug per moles of DNA virions, $d/V = 2.8 \times 10^4$), while a smear indicating a large number of products of varying lengths was observed at higher ratios ($d/P = 20$; $d/V = 1.4 \times 10^5$). Complete destruction of the original DNA was observed at the highest concentrations studied ($d/P = 200$; $d/V = 1.4 \times 10^6$). When compared with the GSH-activated cleavage for the same ratios of drug to DNA, the bc reaction appears to cause less damage, or similar damage for ratios differing by 1 order of magnitude. This difference in reactivity for the two modes of drug activation is expected, since the bc reaction is a slower, more selective reaction that competes less effectively with the spontaneous drug reaction (Figure 1). The GSH activation of NCS chrom is a much faster reaction, and at concentrations of GSH > 50 μM, it effectively completely shuts down the bc spontaneous decomposition at pH ≈ 8.5 (data not shown). Furthermore, the molecular recognition requirements for this reaction are less stringent, as it only requires the presence of a ds region containing a T or A residue for a lesion to occur (Goldberg, 1991, and references therein; Goldberg & Kappen, 1994, and references therein; Stassinopoulos & Goldberg, 1995).

In order to establish the bc nature of the reaction, $\phi\chi$ 174 phage DNA was incubated with NCS chrom in buffers at increasingly higher pH, in 10% MeOH. At pH values between 4 and 10, one could observe a clear increase of the damage between pH = 4 and pH = 8.5, while a decrease in damage was evident for pHs higher than 8.5 (data not shown). This pH dependence is the same as the one observed for small oligonucleotides (Kappen & Goldberg, 1993b). Control experiments showed the $\phi\chi$ 174 DNA to be stable under these pH conditions in the absence of NCS chrom. In a separate control experiment, no cleavage of ds $\phi\chi$ 174 phage DNA was observed under the same conditions, in the absence of GSH, while a standard incubation of NCS chrom with excess GSH and the ds $\phi\chi$ 174 showed the expected (Goldberg, 1991, and references therein; Goldberg & Kappen, 1994, and references therein) production of a mixture containing nicked circular and linear ds DNA products (data not shown).

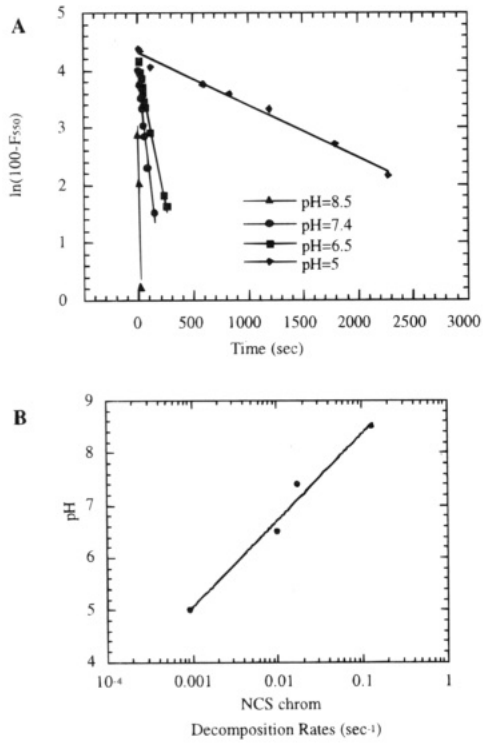

FIGURE 4: (A) Plot of the intensity of fluorescence at 550 nm (λ_{exc} = 400 nm) *vs* time at different pHs (10% MeOH): (▲) 50 mM Tris·HCl (pH = 8.5), (●) 50 mM Tris·HCl (pH = 7.4), (■) 50 mM phosphate (pH = 6.5), and (◆) 50 mM NaOAc (pH = 5). (B) Semilogarithmic plot of the observed rates of decomposition for NCS chrom at different pHs *vs* pH, under pseudo-first order conditions for OH^-.

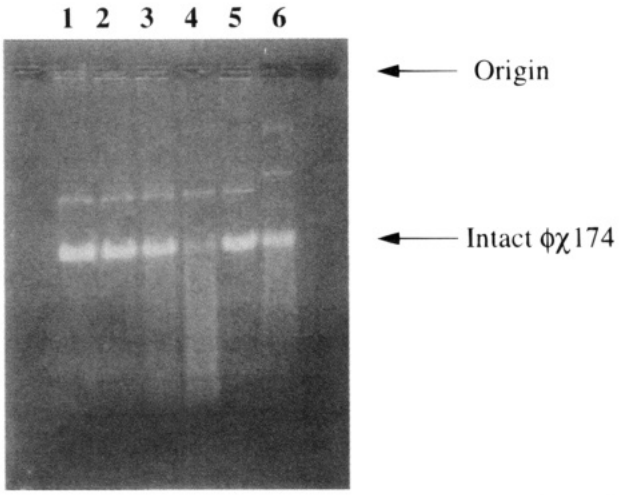

FIGURE 5: Agarose gel electrophoresis of the reaction mixtures for the reaction of 1.5 μg of φχ 174 virion DNA with different concentrations of NCS chrom for 1.5 h at 4 °C, in 50 mM Tris·HCl (pH = 8.5). Lane 1, 0 μM; lane 2, 25 nM; lane 3, 125 nM; lane 4, 1.25 μM; lane 5, 12.5 nM; and lane 6, 25 nM + 5 mM GSH. This 1% gel was run in the presence of 0.5 μg/mL ethidium bromide.

Reaction with Long Single-Stranded DNA Fragments

From the reactivity observed for the circular ss DNAs, it was evident that a significant number of sites existed in DNAs of that length. To test the sequence/structure specificity of this reaction on a piece of DNA long enough to offer significant complexity but sufficiently short to be characterized with base resolution, shorter ss fragments of DNA (I−V, Figure 6A) were synthesized by the use of the PCR reaction, one biotinylated primer (Figure 6B) and pUC19 as a convenient template DNA. These ss fragments were used as DNA substrates with a known sequence and unknown tertiary structure. Under standard conditions, this reaction was found to give only a few (six) distinct lesion sites for the total of these fragments, which sampled the sequence space of ~450 bases. Representative cleavage data are shown in Figure 7A for fragment I (Table 1). Under standard conditions, the reaction was found to give a small number of specific lesions superimposed on a nonspecific background reaction. Lowering of the NCS chrom concentration reduced the nonspecific background concentration, while increasing or keeping constant the intensity of the specific cuts (Figure 7A, compare lanes 2−4). This behavior is reminiscent of the situation for smaller SSOs, for which an optimum concentration is observed for a specific drug:DNA ratio (Figure 3). Under the same conditions, NCS chrom activated by GSH (Figure 7A, lane 6) gave at least 1 order of magnitude more cleavage sites. Furthermore, these sites were mostly located in regions flanking the bc cleavage sites (Figure 7A). The same behavior was observed for SSOs, both in the past and for the present study (*vide infra*). Since the fragments I−IV had the same 3′ sequences (Figure 6A), it was evident that the sites 1−3, observed for the longer fragment I, were also observed in the shorter fragment II. Fragment III did not contain sites 1 and 2 (Table 1), as it is missing the last 100 bases at the 5′ end. The conservation of the same cleavage sites for pieces of different expected secondary structure is consistent with the attack sites' tertiary structure being determined by the immediate sequences flanking the cleavage site, and not being generated by through-space interactions of distant sequences. Since these sites are a result of the interactions of the immediate neighboring sequences, they are expected to be the most thermodynamically stable because of entropy considerations. They will thus stabilize the complex with the hydrogen-abstracting species the most and exhibit maximum cleavage. Alternative folding schemes can, however, stabilize other secondary structures for the same sequences. Fragment V, which contains the sequences including sites 1−3 of fragment I, exhibits strong cutting sites coinciding only with site 2, although most of the flanking sequences for the other sites are present (Figure 6A). Furthermore, a completely new site is found for fragment V (site 6, Table 1).

It is interesting to note that all the cleavage observed for these sequences was at T residues. Most times, the attacked T residues were part of a T-rich sequence (Table 1). This observation includes the original sequences studied (A, B; Table 1). The T preference may reflect either the tendency of the drug to bind and abstract hydrogens from bulged T residues or the thermodynamic stability of bulged structures which contain T residues. In the original study (Kappen & Goldberg 1993a,b), it has been shown that replacement of the attacked bulged T residue by other bases resulted in retention of the residue cleaved with lower but comparable cleavage yields. This observation supports the second explanation for the base selectivity seen.

To test the alkali-catalyzed nature of the cleavage reaction, fragment V was incubated in buffers of different pH under the same concentrations of NCS chrom and percentage of MeOH (Figure 7B). A clear increase of the cleavage was observed as the pH increased from 5 to 9 (Figure 7B, lanes 2−7). At higher pHs, the cleavage yield for most sites was

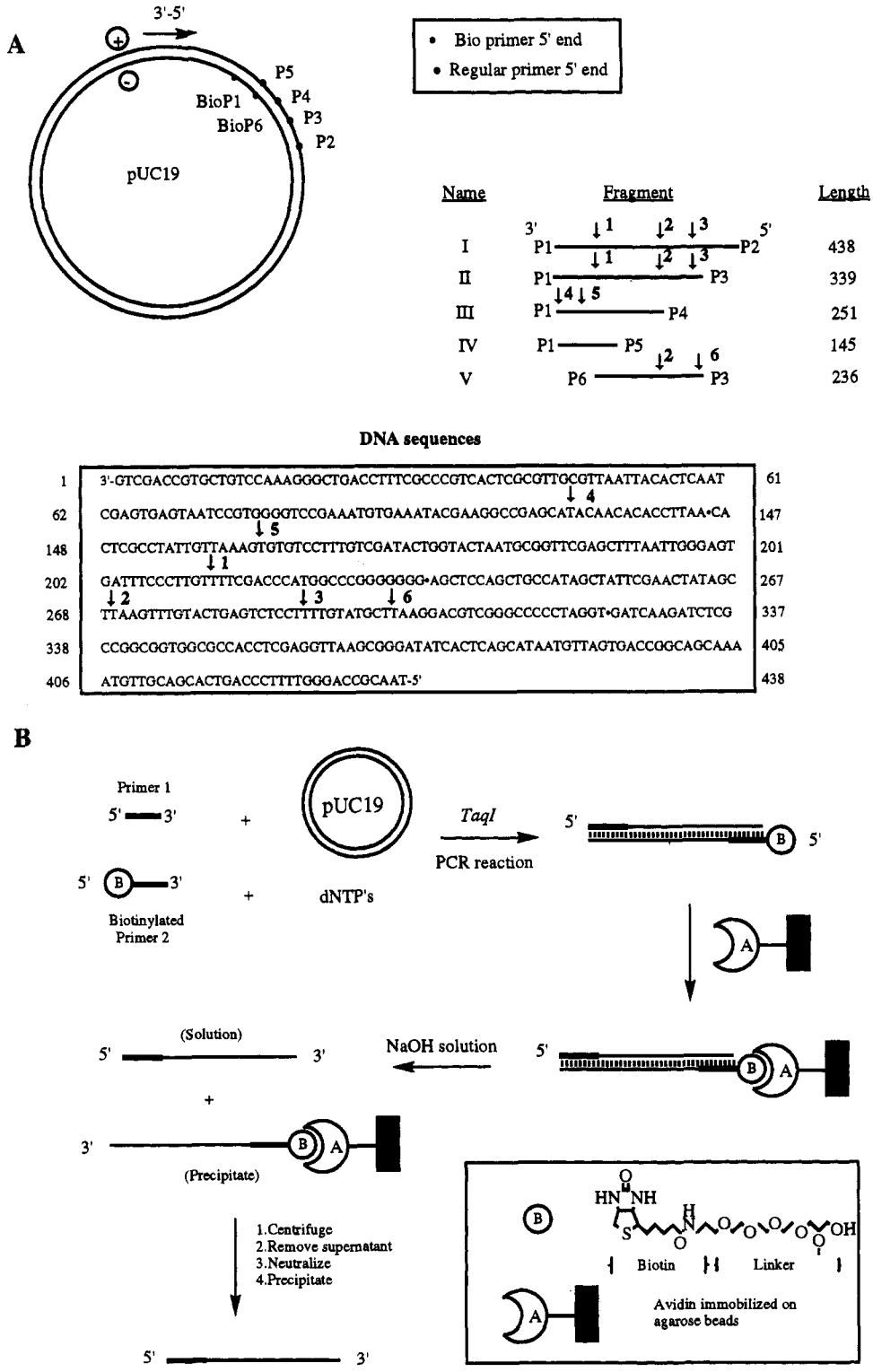

FIGURE 6: (A) Lengths, sequences, and relative compositions of the ss DNA fragments I−V. The circle at the top left shows the relative positions of the primers' 3′ ends on the template pUC19. + corresponds to the strand being isolated, while − corresponds to the complementary biotinylated strands. The arrows in the sequences denote the attacked residues, and ● denotes the end of a fragment. The numbers next to the arrows are the reference numbers for the cleavage sites in Table 1. The entire sequence for the + strand of the template is listed; the numbering scheme is in the 3′ to 5′ direction. (B) Schematic description of the synthesis and isolation of the ss DNA fragments through the use of the PCR reaction. pUC19 is the plasmid used as the template.

quickly decreased as is depicted for site 2 (Figure 7B, lanes 8 and 9; Figure 7C). It is interesting to note that the cleavage at pH = 9 (Figure 7B, lane 7) did not change in terms of cleavage only, but also different sites appeared. This may be because different folding conformers became more favored at that pH, where exchange between different hydrogen-bonding schemes may be more facile.

In order to gain an understanding of the possible secondary structures associated with the ss fragments I−V, we calculated their lowest energy structures by the use of the program MFOLD (Zucker, 1989; Jaeger et al., 1989a,b). Selected lower energy structures calculated for the folding of I−V are shown in Figure 8. The following trends were obvious from this analysis. (a) As expected (Zucker, 1989), several

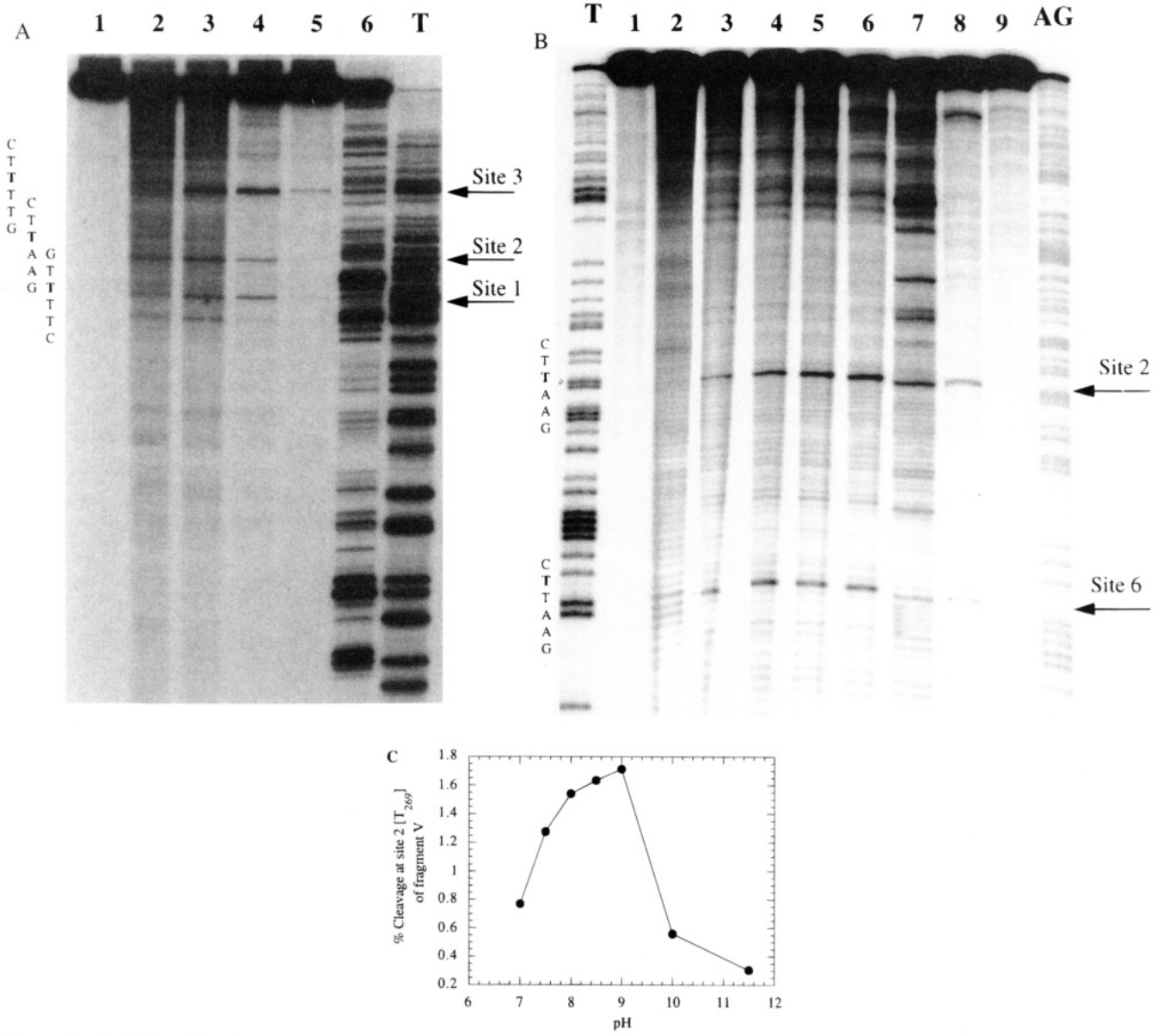

FIGURE 7: (A) Effect of the drug:DNA ratio on the cleavage of fragment I (438 bases). Electrophoresis was on a 4% denaturing polyacrylamide gel. Lane 1: control 5′ end-labeled fragment I in 50 mM Tris·HCl (pH = 8.5) and 10% MeOH. Lanes 2−5: 5′ end-labeled fragment I in the same buffer and MeOH percentage as lane 1, incubated with 39 μM, 3.9 μM, 390 nM, and 39 nM final concentrations of NCS chrom for 1.5 h, respectively. Lane 6 is the same as lane 4 with the additional presence of 5 mM GSH. T corresponds to the Maxam−Gilbert chemical marker. The arrows denote the cleavage sites; numbers correspond to the reference numbers of Table 1. The immediate residues around the target nucleotide are shown on the left side. Attacked residues are in bold. (B) pH dependence of the bc cleavage reaction for the 5′ end-labeled fragment V (236 bases). Electrophoresis was on a 4% denaturing polyacrylamide gel. T and AG denote lanes corresponding to Maxam−Gilbert chemical markers. Lane 1: control 5′ end-labeled fragment V incubated in Tris·HCl (pH = 8.5). Lanes 2−9: 5′ end-labeled fragment V and NCS chrom in buffers of different pH. Lane 2, NaOAc (pH = 5); lane 3, Tris·HCl (pH = 7); lane 4, Tris·HCl (pH = 7.5); lane 5, Tris·HCl (pH = 8); lane 6, Tris·HCl (pH = 8.5); lane 7, glycine (pH = 9); lane 8, glycine (pH = 10); lane 9, glycine (pH = 11.5). Reaction mixtures were incubated at 4 °C for 1.5 h in the dark with 10 μM NCS chrom in 10% MeOH and 50 mM buffer. The arrows denote the cleavage sites; numbers correspond to the reference numbers of Table 1. The immediate residues around the target nucleotide are listed on the left side. Attacked residues are in bold. (C) Plot of the percent of cleavage at site 6 *vs* pH.

different structures are close in energy (within 5−10%) for ss DNA fragments of this size. (b) The cleavage sites (arrows), more often than not, fall within non-ds regions. Since the reaction conditions (low salt and the presence of MeOH), as well as the complexation by the hydrophobic NCS chrom molecule, might change the relative energy order for these structures, it would be unreasonable to expect a perfect prediction of the actual structure from thermodynamic parameters obtained in aqueous solutions containing 1 M NaCl (Zucker, 1989; Jaeger et al., 1989a,b). Furthermore, prediction for structures in loops or other non-ds regions are not easy by any computer program, especially in the absence of any experimental data (Zucker, 1989). As a result, only qualitative conclusions may be drawn from these folding structures.

One should notice that, of all the sites exhibiting bulges or other ss regions, only a small subset gets attacked during the bc reaction, after presumably being recognized by the cleaving species. This indicates that there are specific structural requirements to be met for this drug/ss DNA interaction and demonstrates the importance of the ongoing studies to determine the three-dimensional structure of the complex formed between a stable analog of the drug and the cleavage site through the SSO approach (A. Stassinopo-

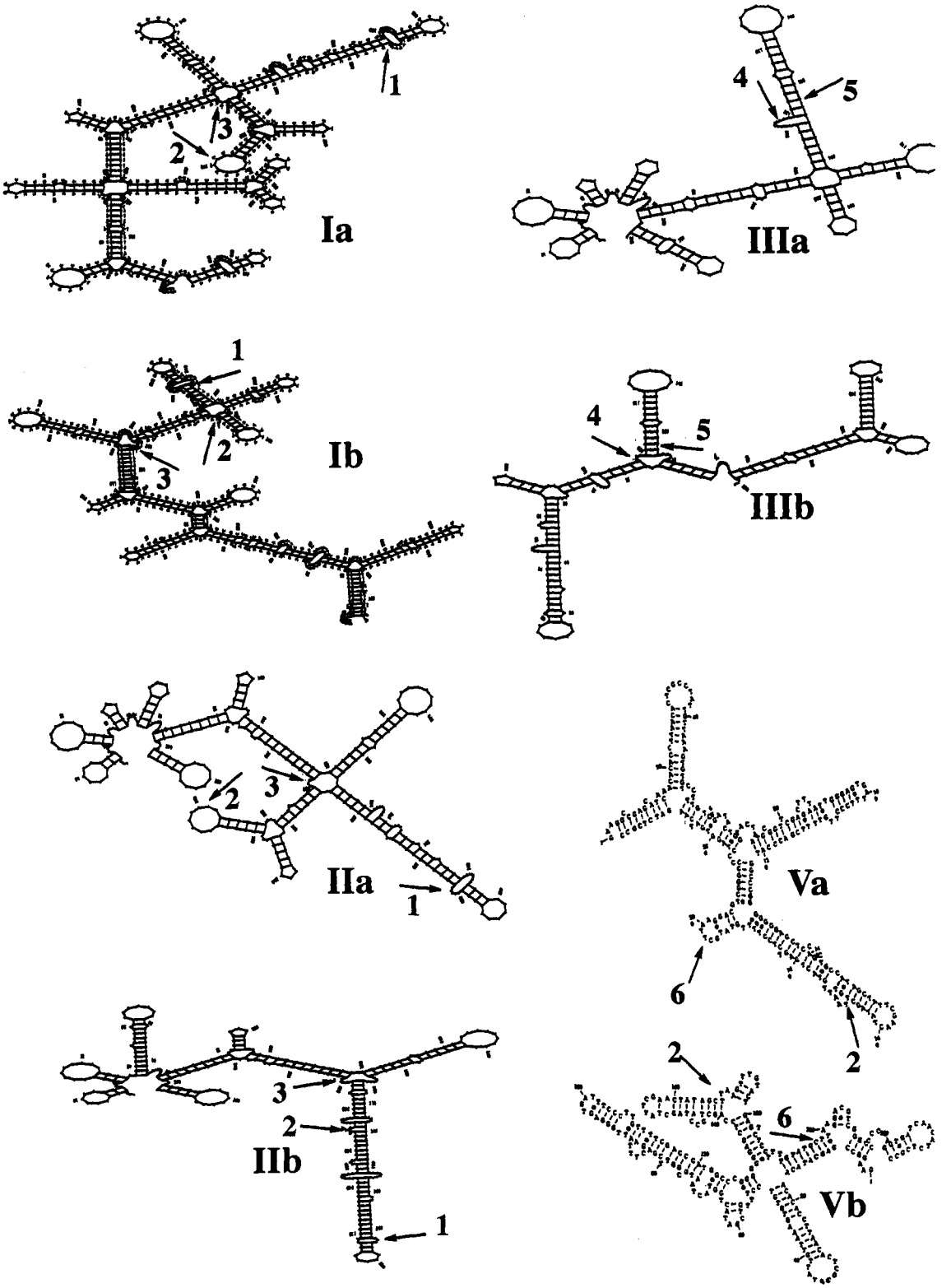

FIGURE 8: Selected folding arrangements from the minimum energy structures calculated by the program MFOLD for the fragments I–III and V (two each). The arrows denote the cleavage sites. The numbers on the arrows correspond to the reference numbers for the sites in Table 1.

ulos, J. Jie, X. Gao, and I. H. Goldberg, unpublished data).

Determining the Minimum Sequence Requirements for One Cleavage Site

The maximum yields of cleavage for the most prominent of these bands were on the order of 1% compared to the total amount of DNA. This low yield is quite reasonable if one considers that, except for the possibility of nonproductive binding sites for the same conformation of these fragments, there is also the possibility of several conformers with similar energies being present simultaneously in solution. If this were true, one would expect truncation of sequences from one or the other end of a longer oligonucleotide containing a cleavage site to result in an increase of the effective

A

Entry	Length		% Cleavage
1	50	AG CTT AAG TTT GTA CTG AGT CTC CTT TTG TAT GCT TAA GGA CGT CGG GCC	2
2	45	CTT AAG TTT GTA CTG AGT CTC CTT TTG TAT GCT TAA GGA CGT CGG	3.5
3	40	CTT AAG TTT GTA CTG AGT CTC CTT TTG TAT GCT TAA GGA C	5.4
4	35	CTT AAG TTT GTA CTG AGT CTC CTT TTG TAT GCT TA	7.9
5	30	CTT AAG TTT GTA CTG AGT CTC CTT TTG TAT	4.0
6	45	G TTT GTA CTG AGT CTC CTT TTG TAT GCT TAA GGA CGT CGG GCC CC	2.8
7	41	GTA CTG AGT CTC CTT TTG TAT GCT TAA GGA CGT CGG GCC CC	2.5
8	36	G AGT CTC CTT TTG TAT GCT TAA GGA CGT CGG GCC CC	2.5
9	21	CTC CTT TTG TAT GCT TAA GGA	0
10	21	G AGT CTC CTT TTG TAT GCT TA	0
11	26	GTA CTG AGT CTC CTT TTG TAT GCT TA	7
12	30	G TTT GTA CTG AGT CTC CTT TTG TAT GCT TA	8
13	19	TA CTG AGT CTC CTT TTG TA	5.9
14	16	TA CTG AGT CTC CTT TT	0
15	17	TA CTG AGT CTC CTT TTG	1.7
16	18	TA CTG AGT CTC CTT TTG T	2.5
17	18	TA C G AGT CTC CTT TTG TA	43
18	18	TA CTG AGT CTC TT TTG TA	27
19	18	A CTG AGT CTC CTT TTG TA	0
20	17	CTG AGT CTC CTT TTG TA	0
21	16	TG AGT CTC CTT TTG TA	0
22	17	TA C G AGT CTC TT TTG TA	51

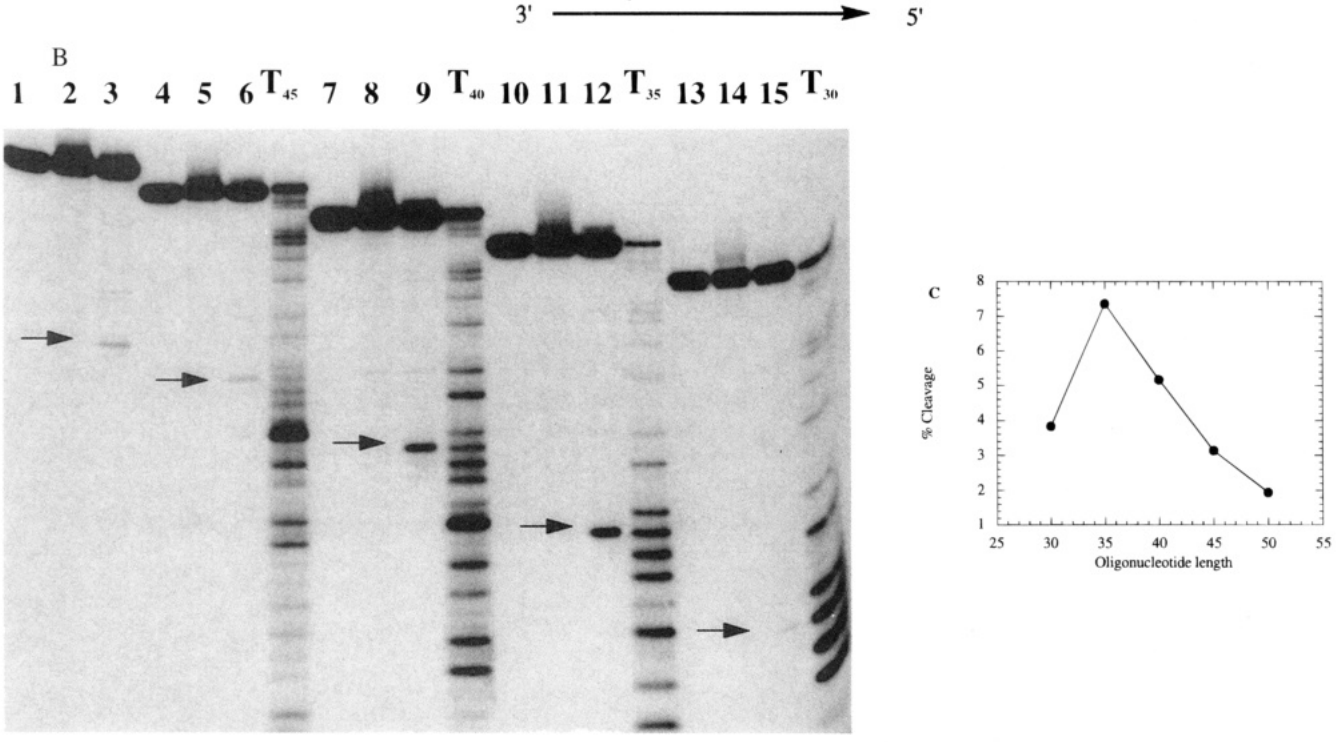

FIGURE 9: (A) Series of oligonucleotides containing site 3 (Table 1) and their maximum cleavage yield under standard conditions [50 mM Tris·HCl (pH = 8.5) and 10% MeOH with a drug:DNA ratio of 2:1]. The cleavage site is indicated by the arrow. (B) Cleavage of oligonucleotides **1**−**4** (Figure 9A) under standard reaction conditions. Electrophoresis was on a 15% denaturing gel. Lanes 1−3 contain 50-mer oligonucleotide (entry 1). Lanes 4−6 contain 45-mer oligonucleotide (entry 2). Lanes 7−9 contain 40-mer oligonucleotide (entry 3). Lanes 10−12 contain 35-mer oligonucleotide (entry 4). Lanes 13−15 contain 30-mer oligonucleotide (entry 5). Lanes 1, 4, 7, 10, and 13 are controls of carrier-free 5′ end-labeled oligonucleotides. Lanes 2, 5, 8, 11, and 14 contain carrier-free 5′ end-labeled oligonucleotides and 10 μM NCS chrom. Lanes 3, 6, 9, 12, and 15 contain radioactive 5′ end-labeled oligonucleotides, 5 μM cold oligonucleotides, and 10 μM NCS chrom. Arrows point out the cleavage bands corresponding to the same T residue. T_n denotes Maxam−Gilbert chemical markers for the oligonucleotide of n length. (C) Plot of the percentage of cleavage at the marked T residue (arrow) *vs* the length of the oligonucleotide in nucleotides (entries 1−5).

concentrations of NCS chrom and cleavage site, while decreasing nonproductive interactions. As a result, increase of the cleavage yield should be observed, so long as the bases participating in the formation and stabilization of the sites are not removed. In order to test this hypothesis, we chemically synthesized a 50-mer oligonucleotide (Figures 9A and 10A; entry 1), containing site 3 (Table 1), which was found to be a substrate for the bc reaction at the same

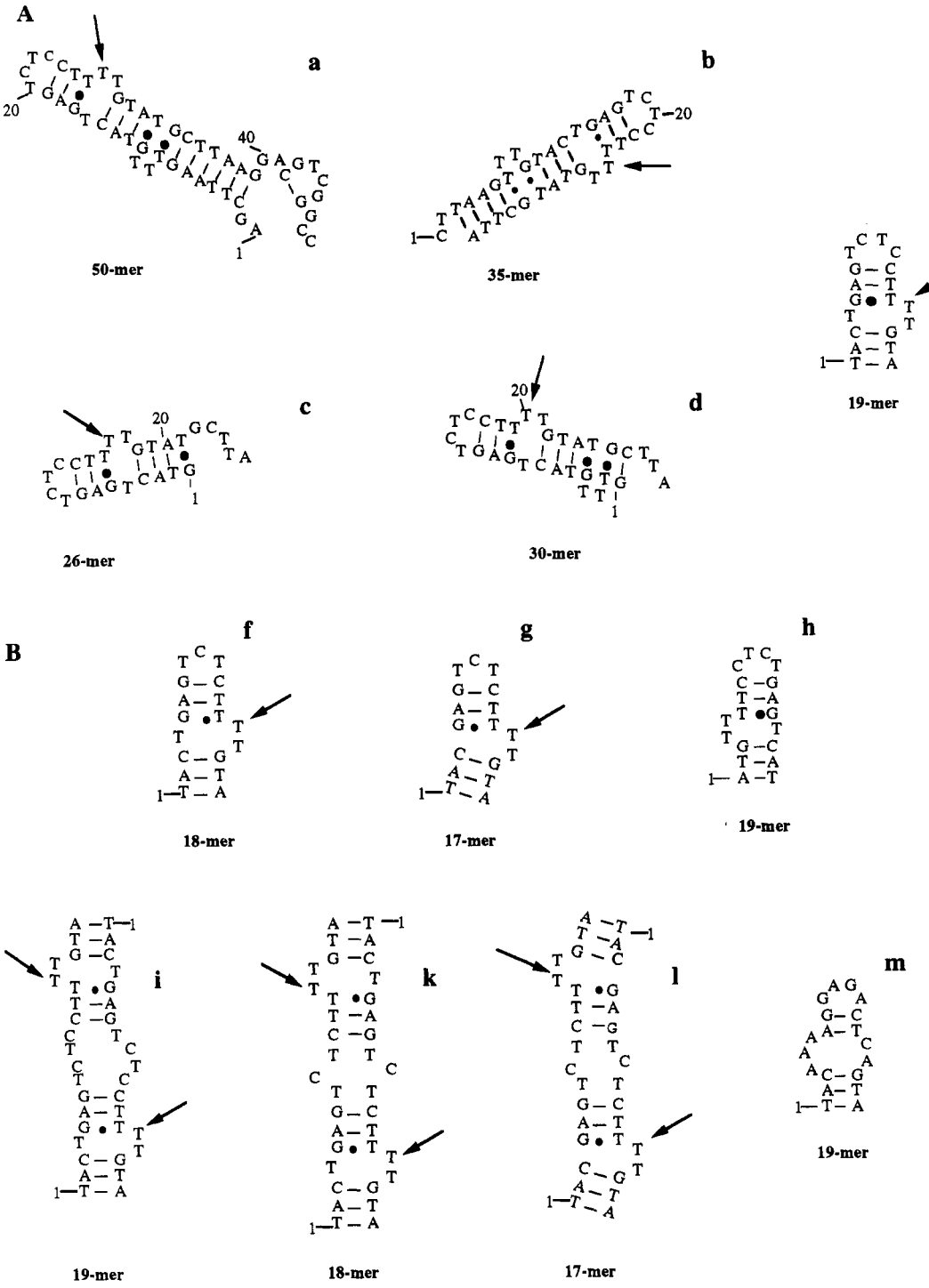

FIGURE 10: (A) Minimum energy secondary structures **a**−**e** of selected oligonucleotides containing site 3. Entries corresponding to Figure 9A are **a** (entry 1), **b** (entry 4), **c** (entry 11), **d** (entry 12), and **e** (entry 13). The numbering scheme for the sequence is in the 3′ to 5′ direction. Arrows denote the cleavage site. A GT-mismatched hydrogen-bonding scheme is indicated by ●. (B) Minimum energy secondary structures **f**−**m** of oligonucleotides related to the oligonucleotide **e** (entry 13) exhibiting optimum cleavage and containing site 3. Structures **f** and **k** correspond to the 18-mer resulting from the removal of the C_{11} residue from the 19-mer, in a monomeric and a dimeric form, respectively. Structures **g** and **l** correspond to the 17-mer resulting from the removal of the T_4 and C_{11} residues, in a monomeric and a dimeric form, respectively. Structures **h** and **m** are the antiparallel and complementary structures of **e**. Structure **f** corresponds to the 19-mer in a dimeric (head-to-tail) arrangement. Entries corresponding to Figure 9A are **f** (entry 18) and **g** (entry 22). The numbering scheme is in the 3′ to 5′ direction. Arrows denote the cleavage site. Lack of arrows indicates a nonsubstrate. A GT-mismatched hydrogen-bonding scheme is marked by ●.

residue. The yield of cleavage for site 3 on this oligonucleotide was higher than for the longer fragments (~2%). Incidentally, the fact that an oligonucleotide synthesized chemically exhibits cleavage at the same site as a fragment generated by the PCR reaction precludes the possibility that the cleavage observed is a PCR reaction artifact. Synthesis of oligonucleotides with truncated sequences at the 3′ and/or 5′ ends resulted in increasing cleavage yields up to the point that further truncation made the cleavage become smaller or disappear (Figure 9B,C; Figure 10A, structures **a**−**d**). Incorporation of the understanding gained for the minimum site requirements on one oligonucleotide, through

these truncation experiments at the 5′ (Figure 9A, entries 2−5) and 3′ (Figure 9A, entries 6−9) ends, yielded an oligonucleotide for which the yield of cleavage was ~6% (Figure 9A, entry 13, and Figure 10A, structure **e**). Further improvement of the cleavage could be obtained by removing features that were thought to destabilize the interactions in the formation of the binding pocket (Figure 9A, entries 17 and 18; Figure 10B, structures **f** and **g**). This resulted in the synthesis of oligonucleotide **22** (Figure 9A, entry 22; Figure 10B, structure **g**), which was the most efficient substrate (cleavage yield, ~51%).

All of these oligonucleotides demonstrated the above-mentioned dependence on the ratio of drug to DNA. As can be seen in figure 9B (e.g., compare lanes 8 and 9), incubation of carrier-free oligonucleotides with NCS chrom shows no significant direct damage, while inclusion of cold oligonucleotide (final drug:DNA molar ratio is 2:1) results in a significant amount of damage.

Since for ss oligonucleotides, the creation of a bulged site requires base-paired regions flanking the site, it is necessary to have a hairpin-type arrangement for these oligonucleotides. Because of their partially self-complementary nature, these oligonucleotides can be either monomeric or dimeric in solution (Figure 10, monomeric **e**−**g**, dimeric **i**−**l**). Because of symmetry considerations, this will not affect the actual site geometry but will affect the stability of the construct and therefore the cleavage yield. To address this issue for the best substrate oligonucleotides, we checked the electrophoretic mobilities under nondenaturing conditions *vs* linear markers of defined length (C_5, C_{10}, C_{20}, C_{30}). A similar test was conducted under the same conditions by Durand et al. (1990) in order to distinguish between a dimeric and monomeric arrangement of an oligonucleotide. We found that all of the substrate oligonucleotides demonstrate mobilities consistent with monomeric arrangements, whether or not an annealing treatment was included before the loading on the gel. This argues in favor of these oligonucleotides being in the monomeric hairpin arrangement (Figure 10, structures **e**−**g**) rather than in the dimeric head-to-tails arrangement (structures **i**−**l**). It is, however, possible that, under the conditions of the native polyacrylamide gel, the equilibrium of the dimeric and monomeric forms has been disturbed and what is observed is not the situation in the reaction solution. For the longer pieces of DNA, nonetheless, ss circular phage DNA or the fragments I−V, and in the very low concentrations that were used during their cleavage experiments, one would not expect the facile formation of a dimeric structure at these sites, especially since annealing did not seem to affect either the yield or the outcome of the reaction (data not shown).

Finally, for the best substrate containing the intact site 3 oligonucleotide, the antiparallel and complementary arrangements for that sequence (Figure 10B, structures **h** and **m**) were synthesized and tested as substrates. Neither arrangement was found to be a substrate for the bc reaction. In contrast to our finding for the site 3-containing oligonucleotides, the complementary oligonucleotide for site A (Table 1) SSOs was found to be cleaved under the same conditions, although with a smaller yield (2:1) (Kappen & Goldberg, 1993b). The origin of this difference can be traced to the fact that the site 3 arrangement of the site is an asymmetric one, while the one of site A is symmetric. As a result, while the mirror image folding of site A oligonucleotide may interact in a similar fashion with the cleaving form of NCS chrom, this is not a possibility for site 3 (Figure 10B, structure **h**).

HPLC analysis of the drug final products after the cleavage reaction for the 17-mer oligonucleotide (entry 22, Figure 9) [1.5 h, 4 °C, 50 mM Tris·HCl (pH = 8.5); 10% MeOH; 1:1 NCS chrom:DNA] revealed the formation of a product with the same retention time as product **8** and reduced formation of the spontaneous decomposition products **7** and **7a**. Isolation of the fraction corresponding to that peak and coinjection with an authentic sample of **8** confirmed it to be the same compound (data not shown).

Base-Catalyzed Drug Reaction with RNA

The ss RNA can form tertiary structures similar to those of ss DNA, and furthermore, the ss form of RNA is physiologically more abundant than ss DNA, playing structural, regulating, and catalytic roles in all higher organisms (Nagai & Mattaj, 1994, and references therein). We decided, therefore, to test whether the bc reaction of NCS chrom can be used for the specific cleavage of ribonucleic acids at bulged residues. We chose to use the sequence of fragment II, for which we have characterized the reactivity in the case of ss DNA. By the use of the T7 polymerase runoff translation system and a PCR-amplified ds DNA fragment as a template, we synthesized and tested an RNA 339-mer featuring the same sequence as fragment II (Figure 6A). Upon reaction with NCS chrom under standard pH and MeOH percentage, we found no cleavage above background for a variety of conditions and NCS chrom concentrations.

The ss DNA and ss RNA of the same sequence will have different tertiary structures, especially for the ds regions (Tinoco et al., 1987, 1990; Draper, 1992, and references therein). For large pieces of either DNA or RNA (>100 bases long), one would expect populations of several different species with similar energies (within 5−10%) to be present in solution as part of an equilibrium. For two long pieces with the same sequence, one RNA the other DNA, one would expect at least partial overlap of the secondary structures of some of the species from one population with some from the other. Results supporting this idea have been collected by several groups, showing functions of ss DNAs similar to those of their counterpart ss RNAs in places where it implied at least partial overlap of the structures (Khan & Roe, 1989; Perreault et al., 1989; Paquette et al., 1989; Holmes & Hecht, 1993). If one assumes that the requirements for a cleaving site of NCS chrom through the bc reaction are determined by the secondary structure, e.g., the formation of a bulge, one might expect to find similar cutting for comparable sites in both DNA and RNA. This was not observed in the case of fragment II. Consistent with this finding are recent results obtained for the cleavage yields of TAR RNA and its DNA analog (site B, Table 1) by NCS chrom (Kappen & Goldberg, 1995). In that study, only a small percentage (~5%) of the DNA cleavage yield was observed for an oligoribonucleotide of the same sequence. Given the weak cleavage of sites on long ss DNA fragments (1%), this puts the expected yields at levels (0.005%) too low to observe in the presence of the background ribonuclease cleavage found for labeled RNAs.

In an attempt to detect even a very weak reaction with ribonucleic acids at specific sites, we chemically synthesized

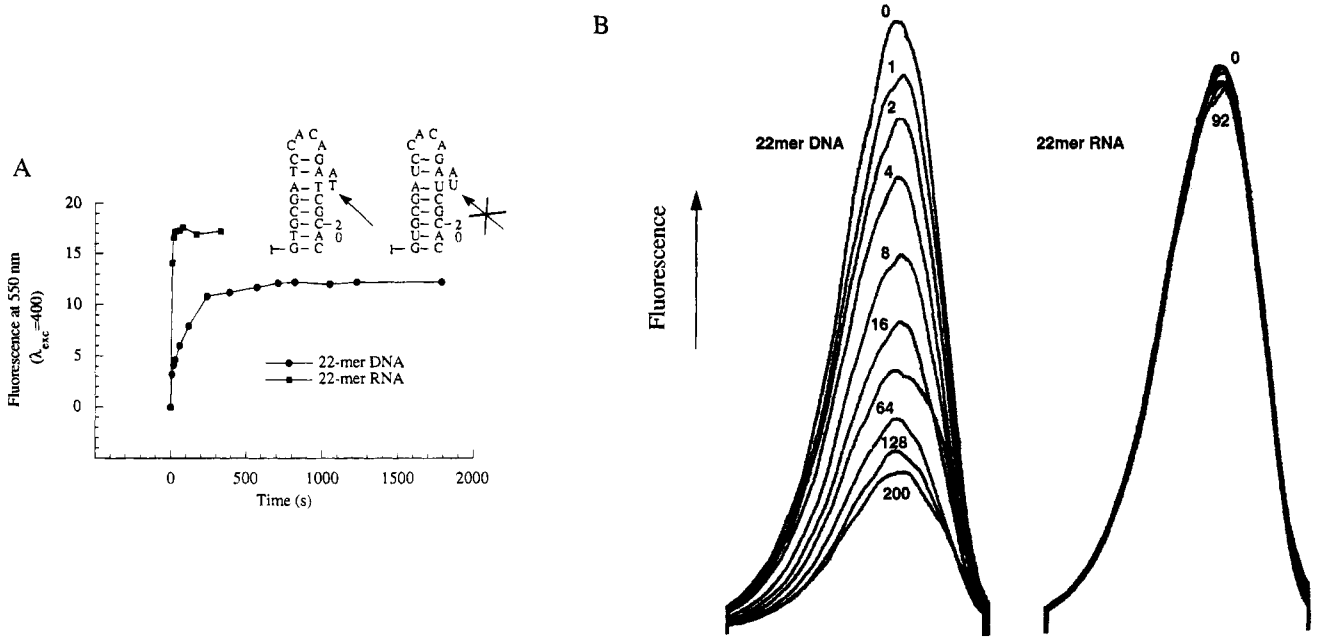

FIGURE 11: (A) Plot of fluorescence at 550 nm (λ_{exc} = 400 nm) *vs* time of incubation for mixtures containing 1 equiv of NCS chrom and 2 equiv (oligonucleotide) of the 22-mer DNA (●) or RNA (■). Maximum fluorescence intensity is at 500 nm. Reaction conditions: 2 °C, 50 mM Tris·HCl (pH = 8.5), 5% MeOH, and 5 μM NCS chrom. The insert shows the predicted lowest energy secondary structures. Arrows show the residue attacked. (B) Emission fluorescence spectra (λ_{exc} = 400 nm) of **7** upon addition of the 22-mer DNA (left) or 22-mer RNA (right) at 2 °C, 25 mM NaOAc (pH = 5.2), and 5% MeOH. The numbers denote the volume in microliters of a stock solution of the respective oligonucleotide added. Final [**7**] = 1 μM. The stock concentration for 22-mer oligonucleotides is 470 μM.

and tested the minimal 17-mer oligoribonucleotides (entry 22, Figure 10A) as an analog of site 3 and a 22-mer oligoribonucleotide containing the site A (Table 1) found in the past to give high cleavage yield for DNA (Yang et al., 1995). Again, no cleavage above background was observed for either. These results were more unexpected as the high cleavage yield of these DNA substrates (70−80%) would have put them within the detection range of the experiment even for the weaker RNA cleavage yields, if one assumes that there is a fixed yield ratio between a DNA and an RNA site of the same sequence. Reaction in the presence of GSH also gave no cleavage above background, as was also reported recently (Kappen & Goldberg, 1995).

Kinetic and Binding Spectroscopic Studies with RNA Molecules

In order to determine the basis for the difference between the interactions of NCS chrom with a deoxyribonucleotide substrate of the bc reaction and a ribonucleotide of the same sequence, we decided to use the same 22-mer oligonucleotide sequence identified by our previous studies to be an excellent DNA substrate by virtue of a very stable structure (Figure 11A, insert) (Yang et al., 1995). The stability of this structure is the result of a 6-base pair apical stem.

When an equimolar amount of native drug and 22-mer DNA were incubated at 2 °C, the expected slow fluorescence increase, diagnostic of the bc formation of **8**, was observed (Figure 11A). When, however, the same experiment was conducted with the 22-mer RNA of identical sequence, a fast fluorescence increase at 550 nm, diagnostic of the formation of **7**, was observed through the spontaneous decomposition reaction. Indeed, when NCS chrom was incubated alone under the same conditions, an identical fast increase of the fluorescence at 550 nm was observed (Figure 2). Given the reaction characteristics outlined in Figure 1, these observations indicate that the NCS chrom-derived binding species (cumulene **5** or biradical **6**) does not form a stable complex with the cleavage site. HPLC of the three spent mixtures that were used for the fluorescence experiments confirmed that only in the case of the 22-mer DNA was **8** produced. The other two mixtures gave identical mixtures of products containing mostly **7** and some **7a**. These HPLC data also eliminate the possibility that the RNA 22-mer might be acting as a ribozyme, producing **8** with a fast rate, but not getting cleaved in the process.

A binding assay for the postactivated form **7** was also conducted with the two 22-mer oligonucleotides. This assay has been shown to be a reliable measure of whether a certain oligonucleotide is a substrate for the bc reaction, since **7** can be considered to be a structural analog of the biradical **6**, which, in either one or two steps, is the most likely species ultimately responsible for the hydrogen abstraction from the substrates (Yang et al., 1995). Furthermore, **7** is expected to have the same general shape as the base-generated cumulene **5** (a species possibly involved in the site-selective binding), since in both the C1″−C12 bond has been formed and the spirolactone five-membered ring has locked the conformation of the two planar systems at a particular angle (34.2°).

Incubation of **7** with increasing amounts of the DNA 22-mer showed a marked decrease in its fluorescence intensity at 500 nm, consistent with a binding constant of 2.9 μM (Figure 11B, left) (Yang et al., 1995). Incubation of **7** with increasing amounts of the 22-mer RNA on the other hand had a minimal effect on the fluorescence intensity, indicating no binding (Figure 11B, right).

Both the kinetic and the thermodynamic assays outlined above seem to indicate that there is no formation of a stable RNA-cleaving species complex, as is the case for the DNA, and that the native NCS chrom seems, instead, to decompose

following the spontaneous decomposition pathway (Figure 1). These results preclude the possibility that the main reason behind the observed higher stability of RNA toward NCS chrom is that its chemical alteration may lead to one or more products that cannot be detected by electrophoretic analysis (Holmes & Hecht, 1993). These results point to differences in the detailed tertiary structure of RNA under the reaction conditions for the observed difference in DNA and RNA reactivity.

CONCLUSIONS

As was shown earlier, NCS chrom will cleave at specific bulged sequences of oligonucleotides upon incubation at basic pH (Kappen & Goldberg, 1993a,b, 1995). In order to test whether this reaction can be used as a probe for bulged structures in long ss nucleic acids, we tested larger ss DNAs, which are found in the infectious form of some phages (virions) (Denhardt et al., 1978) as substrates. The ss circular forms of $\phi\chi$ 174 and the M13 phage DNA were used as substrates of defined sequence and unknown tertiary structure. Their large sizes (5000 and 7500 bases) guaranteed the existence of a significant number of cleavage sites, and their circular nature ensured an easy detection of cleavage because of the expected change in electrophoretic mobility. They were found to be substrates of the bc reaction and to show the same pH and drug concentration dependence on the degree of damage they received, as small oligonucleotides substrates for the bc reaction. Further, synthesis of five ss DNA fragments by the PCR reaction with sizes between 150 and 450 bases showed four of them to satisfy the molecular recognition requirements for the bc reaction-cleaving species at six sites. Since the ss DNAs I−III (Figure 6A) had overlapping 3′ sequences, it was apparent that some sites were observed in all of them, as long as the sequence where the cleavage occurred was present. This indicates that the structure responsible for the recognition/cleavage by the chromophore is a result of the immediate neighboring residues and not formed by remote sequences of the molecule which come together upon folding. Upon reaction of the same sequences with NCS chrom in the presence of thiol, reactivity mostly in regions flanking the one involved in the bc reaction was observed. The damage observed with GSH activation had lower specificity but higher reactivity for the same chromophore concentration.

In order to determine what type of secondary structure is associated with the cleavage sites, we calculated the predicted lowest energy secondary structures for pieces I−V by the use of the program MFOLD (Zucker, 1989; Jaeger et al., 1989a,b). We found that, for several of the lowest energy predicted secondary arrangements, the cleavage sites coincided with non-ds sections of the molecule, where there was either a multiple base bulge or the beginning of a looped structure for which a structure cannot be accurately predicted by this program, especially under the low salt conditions used (Figure 8). For all pieces, several structures existed which have very similar energies (differing by <5%) and should thus coexist in solution. The relatively large size of these molecules will also be responsible for the generation of other nonproductive binding sites that will compete with the productive sites for NCS chrom. Since NCS chrom has a limited lifetime in the absence of a bulged DNA site (Figure 1), the above explanations can account for the low cleavage yields observed and predict that only sites with a significant binding affinity/thermodynamic stability will be cleaved. Chemical synthesis and minimization/optimization of the DNA size for one of the cleavage sites further proved these sites to satisfy the five criteria found for the bc reaction on small oligonucleotides.

(a) The reaction must show increased reactivity at more alkaline pHs, where the chromophore can undergo the bc transformation in Scheme 2. (b) The concentration profile of the reactivity must exhibit an optimum concentration as is the case for the smaller oligonucleotides that contain one cleavage site. (c) The cleavage must take place at a nonduplex region. (d) The rates of the chromophore activation/cleavage reaction should be slower, when compared with the rates of the glutathione-dependent reaction or the spontaneous decomposition in alkaline pH and absence of DNA. (e) The formation of product **8** is associated with cleavage.

Testing of the bc reaction for a long ss RNA fragment of 339 bases or oligoribonucleotides containing the optimized sites for DNA cleavage (22, 19-mers) showed them not to be cleavage substrates. Spectroscopic studies on RNA and DNA oligonucleotides of the same sequence further demonstrated that this depended on binding of the reactive drug species to the nucleic acid. Since the secondary structures of these oligonucleotides are expected to be similar, this is consistent with the tertiary structure of RNA being responsible for this lack of binding.

Although the bc reaction of NCS chrom with ss DNA of large size shows promise as a means of identification of specific substructures within the tertiary structure through molecular recognition and cleavage, the exact requirements for this selection are not completely deciphered. A higher resolution understanding of the interactions through the structural analysis of the complex formed between an SSO and a stable drug analog will be of help. An approach along these lines is already under way (A. Stassinopoulos, J. Jie, X. Gao, and I. H. Goldberg, unpublished data).

ACKNOWLEDGMENT

We thank Dr. Bernard Cuenoud (MGH) for the synthesis of the first biotinylated primer and for his help and expert advice in the synthesis of the long ss DNA fragments by the PCR methodology as well as synthesis and handling of the RNAs. We thank Dr. Lizzy Kappen for her expert advice on the bc reaction and for samples of the oligonucleotides 19-I and 19-II.

REFERENCES

Ausubel, F. M., Brent, R., Kingston, R. E., Moore, D. D., Seidman, G. G., Smith, J. A., & Struhl, K. (1989) *Current Protocols in Molecular Biology*, John Wiley & Sons, New York.

Cantor, C. R., & Warshaw, M. M. (1970) *Biopolymers 9*, 1057.

Dedon, P. C., & Goldberg, I. H. (1992) *Biochemistry 31*, 1909.

Denhardt, D. J., Dressler, D., & Ray, D. S., Eds. (1978) *The ss DNA phages*, Cold Spring Harbor Laboratory, Cold Spring Harbor, NY.

Draper, D. E. (1992) *Acc. Chem. Res. 25*, 201.

Durand, M., Chevrie, K., Chassignol, M., Thuong, N. T., & Maurizot, J. C. (1990) *Nucleic Acids Res. 18*, 6353.

Gao, X., Stassinopoulos, A., Rice, J. W., & Goldberg, I. H. (1995a) *Biochemistry 34*, 40.

Gao, X., Stassinopoulos, A., Gu, J., & Goldberg, I. H. (1995b) *Bioorg. Med. Chem. 3*, 795.

Goldberg, I. H. (1991) *Acc. Chem. Res. 24*, 191.

Goldberg, I. H., & Kappen, L. S. (1994) in *Enediyne Antibiotics as Antitumor Agents* (Borders, D. B., & Doyle, T. W., Eds.) p 327, Marcell Dekker, Inc., New York.
Hensens, O. D., Dewey, R. S., Liesch, J. M., Napier, M. A., Reemer, R. A., Smith, J. L., Albers-Schoenberg, J., & Goldberg, I. H. (1983) *Biochem. Biophys. Res. Commun. 113*, 538.
Hensens, O. D., Helms, G. L., Zink, D. L., Chin, D.-H., Kappen, L. S., & Goldberg, I. H. (1993) *J. Am. Chem. Soc. 115*, 11030.
Hensens, O. D., Chin, D.-H., Stassinopoulos, A., Zink, D. L., Kappen, L. S., & Goldberg, I. H. (1994) *Proc. Natl. Acad. Sci. U.S.A. 91*, 4534.
Holmes, C. E., & Hecht, S. M. (1993) *J. Biol. Chem. 268*, 25909.
Ishida, N., Miyazaki, K., Kumagai, K., & Rikimaru, M. (1965) *J. Antibiot., Ser. A 18*, 68.
Jaeger, J. A., Turner, D. H., & Zucker, M. (1989a) *Methods Enzymol. 183*, 281.
Jaeger, J. A., Turner, D. H., & Zucker, M. (1989b) *Proc. Natl. Acad. Sci. U.S.A. 86*, 7706.
Kahn, A. S., & Roe, B. A. (1989) *Science 24*, 74.
Kappen, L. S., & Goldberg, I. H. (1992a) *Proc. Natl. Acad. Sci. U.S.A. 89*, 6706.
Kappen, L. S., & Goldberg, I. H. (1992b) *Biochemistry 31*, 9081.
Kappen, L. S., & Goldberg, I. H. (1993a) *Science 261*, 1319.
Kappen, L. S., & Goldberg, I. H. (1993b) *Biochemistry 32*, 13138.
Kappen, L. S., & Goldberg, I. H. (1995) *Biochemistry 34*, 5997.
Kim, K.-H. K., Kwon, B.-M., Myers, A. G. & Rees, D. C. (1993) *Science 262*, 1042.
Milligan, J. F., Groebe, D. R., Witherell, G. W., & Uhlenbeck, O. C. (1979) *Nucleic Acids Res. 15*, 8754.
Myers, A. G. (1987) *Tetrahedron Lett. 28*, 4493.
Myers, A. G., & Proteau, P. J. (1989) *J. Am. Chem. Soc. 111*, 7212.
Nagai, K., & Mattaj, I. W., Eds. (1994) *RNA-Protein Interactions*, Oxford University Press, New York.
Napier, M. A., & Goldberg, I. H. (1983) *Mol. Pharmacol. 23*, 500.
Paquette, J., Nicoghosian, K., Qi, G., Beauchemin, N., & Cedergren, R. (1990) *Eur. J. Biochem. 189*, 259.
Perreault, J. P., Pon, R. T., Jiang, M., Usmav, N., Pika, J., Ogilvie, K. K., & Cedergren, R. (1989) *Eur. J. Biochem. 186*, 259.
Povirk, L. F., & Goldberg. I. H. (1980) *Biochemistry 19*, 4773.
Stassinopoulos, A., & Goldberg, I. H. (1995) *Bioorg. Med. Chem. 3*, 713.
Tinoco, I., Jr., Davis, P. W., Hardin, C. C., Puglisi, J. D., Walker, G. T., & Wyatt, J. (1987) *Cold Spring Harbor Symp. Quant. Biol. 102*, 135.
Tinoco, I., Jr., Puglisi, J. D., & Wyatt, J. (1990) in *Nucleic Acids and Molecular Biology* (Eckstein, F., & Lilley, D. M. J., Eds.) Vol. 4, p 205, Springer-Verlag, Berlin.
Williams, L. D., & Goldberg, I. H. (1988) *Biochemistry 27*, 3005.
Yang, C. F., Stassinopoulos, A., & Goldberg, I. H. (1995) *Biochemistry 34*, 2267.
Zucker, M. (1989) *Science 244*, 48.

BI951802N